ACS APPLIED MATERIALS & INTERFACES

Research Article

www.acsami.org

Pseudocapacitive Properties of Two-Dimensional Surface Vanadia Phases Formed Spontaneously on Titania

Mojtaba Samiee and Jian Luo*

Department of NanoEngineering, Program of Materials Science and Engineering, University of California, San Diego, La Jolla, California 92093-0448, United States

Supporting Information

ABSTRACT: Pseudocapacitive properties of V_2O_5-based adsorbates supported on TiO_2 nanoparticles, which form spontaneously as two-dimensional (2-D) nonautonomous surface phases (complexions) at thermodynamic equilibria, have been systematically measured. Surprisingly, surface amorphous films (SAFs), which form naturally at thermodynamic equilibria at 550−600 °C with self-regulating or "equilibrium" thicknesses on the order of 1 nm, exhibit superior electrochemical performance at moderate and high scan rates (20−500 mV/s) that are of prime importance for supercapacitor applications, as compared with submonolayer and monolayer adsorbates formed at lower equilibration temperatures. This study suggests a new direction to design and fabricate a novel class of supercapacitors and other functional devices via utilizing 2-D interfacial phases that can form spontaneously via facile, cost-effective, and highly scalable synthesis routes.

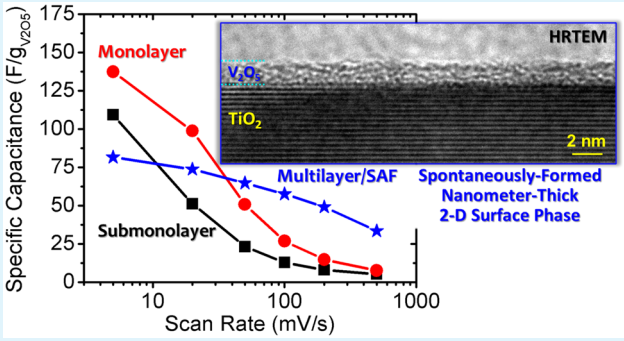

KEYWORDS: *pseudocapacitors, surface amorphous film (SAF), submonolayer, monolayer, vanadium oxide, symmetric supercapacitor*

1. INTRODUCTION

Nanoscale surface engineering via the spontaneously formed two-dimensional (2-D) surface phases (that were also named as "complexions" based on arguments that they are not Gibbs phases rigorously and cannot exist by themselves without the supporting bulk phases[1]) is emerging as a facile and generic method to improve the performance of a variety of functional materials for energy related applications, including lithium-ion batteries,[2−5] oxygen-ion conducting nanowires,[6] and photocatalysts.[7,8] Classical examples of 2-D surface phases (complexions) are represented by monolayer and multilayer surface adsorbates that form spontaneously at thermodynamic equilibria. At high temperatures, surface adsorption can often occur in conjunction with premelting-like surface disordering; in this regard, the formation of a class of adsorbate-based surface amorphous films (SAFs) with self-selecting (equilibrium) thickness on the order of 1 nm, which form from coupled surface premelting and prewetting transitions, have been found in numerous oxide systems.[9] Thermodynamically, such 2-D surface phases (complexions) can possess structures and compositions that differ markedly from any bulk phases (e.g., SAFs are neither fully amorphous nor completely crystalline, despite they are called "amorphous" films; moreover, their average compositions can lie in the bulk miscibility gaps);[9] because they can possess atomic structure and chemistry that are neither observed nor necessarily stable as bulk phases, such 2-D surface phases can have distinct properties unattainable by any bulk phases.

Specifically, this study explores the feasibility of using 2-D surface adsorbates as a novel and economic class of pseudocapacitors, where the charge storage is based on fast surface redox reactions that occur only on the surfaces or in the near-surface regions. Here, a key technological motivation is that such 2-D surface phases can form spontaneously upon a facile "mixing and annealing" process, so that the synthesis and fabrication are cost-effective and scalable. Moreover, understanding the pseudocapacitive properties of 2-D surface adsorbates (as a class of nonautonomous surface phases), which are in principle distinct from any bulk or conventional nanomaterials, is scientifically interesting and significant.

On one hand, there was already some evidence that surface modification can significantly affect the specific capacitance of carbon-based electric double layer capacitors.[10,11] On the other hand, supported oxide catalysts, where the "monolayer" adsorption of catalytic species, such as V_2O_5 and MoO_3, on a high-surface-area nanoparticles of supporting oxides, such as TiO_2 and Al_2O_3, have been widely used in the petroleum, chemical, and environmental industries.[12−17]

Inspired by a supported monolayer catalyst (V_2O_5 on TiO_2), Epifani et al. recently reported that the submonolayer adsorption of VO_4^{3-} species on the surfaces of TiO_2 increases the voltage window, specific capacitance, and cycling stability of

Received: March 24, 2016
Accepted: May 4, 2016
Published: May 4, 2016

DOI: 10.1021/acsami.6b03569
ACS Appl. Mater. Interfaces 2016, 8, 12871−12880

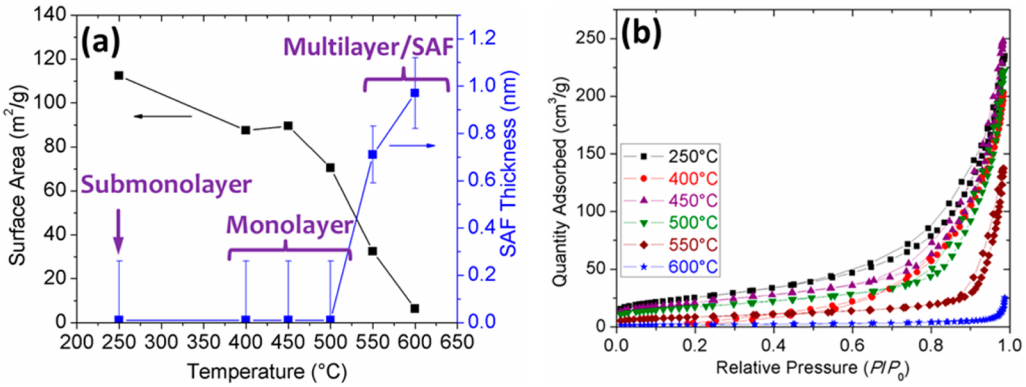

Figure 1. (a) Measured BET surface areas and the thicknesses (or equivalent thicknesses) of the 2-D vanadia phases formed on the surfaces of TiO_2 nanoparticles vs annealing/equilibration temperatures. For specimens annealed at 500 °C or lower, the 2-D surface vanadia phases are not discernible in HRTEM (<0.3 nm); the corresponding horizontal bars represent the equivalent thicknesses calculated from the nominal surface coverages of V listed in Table 1, assuming (for simplicity) that the density of 2-D surface vanadia phase is identical to that of bulk V_2O_5; (b) Nitrogen adsorption−desorption plots for specimens annealed at different temperatures.

the capacitive performance, as well as the electrical conductivity of the material.[18] Because the capacitance of pure TiO_2 is <1 F/g at 5 mV/s, the measured capacitance was attributed to the surface vanadia-based species,[18] which should be at submonolayer levels based on the low annealing temperature of 250 °C.[12−17] These supported submonolayer vanadia catalysts can be considered as one (traditional) class of 2-D surface complexions, whose catalytic properties are modified by the interactions with the underneath metal oxide support. Epifani et al. adopted a low annealing temperature of 250 °C to form submonolayer vanadia adsorbates. A series of recent studies further demonstrated that nanoscale SAFs (disordered multilayer adsorbates) of equilibrium thicknesses on the order of 1 nm will form spontaneously at thermodynamic equilibria at temperatures >500 °C.[19,20] These nanoscale SAFs exhibit a self-limiting (equilibrium) thickness that is independent of synthesis procedures (equilibration time and the excess amount of V_2O_5, once the equilibrium was reached) but reversibly depends on the equilibration temperature.[19,20] It is scientifically interesting to investigate the pseudocapacitive properties of different types of 2-D surface phases, which is one major motivation of this study.

This present study investigated the electrochemical properties of three different types of 2-D surface vanadia phases, with a focus on surface complexions with higher levels of surface adsorptions and disorder that form at higher temperatures with significantly improved performance at moderate and high scan rates; in addition, this study measured the capacitances at a broader range of scan rates than those in the prior study.[18] Specifically, this study showed that the vanadia based surface monolayers, the typical supported catalysts used in the petroleum industry,[12−17] exhibit higher overall capacitance than submonolayer adsorbates reported by Epifani et al.,[18] even with the reduced surface areas due to higher annealing temperatures. More surprisingly, the nanoscale SAFs (disordered multilayer vanadia) that formed at even higher temperatures exhibit better electrochemical performance at moderate and high scan rates of 50−500 mV/s, which are of prime importance for supercapacitor applications, despite drastic reductions in surface areas. In a broader context, these findings suggest new opportunities to design and cost-effectively fabricate a novel class of supercapacitors via utilizing on 2-D surface adsorbates that can form spontaneously via facile and scalable synthesis routes.

2. EXPERIMENTAL PROCEDURE

2.1. Preparation of V_2O_5 Coated TiO_2. TiO_2 anatase powders (~10 nm, 99.99%) were purchased from MTI Corporation (Richmond, CA) and annealed at 250 °C for 4 h to remove moisture. Ammonium vanadate precursor (NH_4VO_3, 99.995%) was purchased from Alfa Aesar. The samples were prepared following a previous report.[19] Briefly, anatase powder was impregnated with a mixed solution of NH_4VO_3 and NH_4OH, and the mixtures were dried at 80 °C overnight. The dried specimens were annealed at 250, 400, 450, 500, 550, and 600 °C, respectively, for 4 h in a closed container to form submonolayer, monolayer and SAFs, and air quenched subsequently. After annealing, excess V_2O_5-enriched secondary phase form large flakes, which were carefully removed before characterization and electrochemical measurements. The overall composition of the remaining powder (without the secondary phase) was measured.

2.2. Characterization. The phase and crystallite size of the samples were evaluated by X-ray diffraction (XRD) using a Rigaku Rotaflex diffractometer with Cu K_α radiation (K_{α_1} = 1.54056), operating at 40 kV and 100 mA. Particle sizes were determined from XRD peak broadening using the Scherrer equation. A LaB_6 standard sample was used to remove the instrumental broadening. The BET surface areas of the powders were determined by nitrogen adsorption using Tristar 3000 (Micromeritics Instruments Corp.). The samples were degassed at 200 °C for 4 h prior to nitrogen adsorption−desorption measurements. The elemental analysis was performed by inductively coupled plasma-optically emission spectroscopy (ICP-OES) using a PerkinElmer 3700 optical emission spectrometer to determine the actual loading of vanadium. Typically, 20 mg of the sample was dissolved in concentrated acidic solution containing HF, H_2SO_4, and H_2O_2. Finally, the obtained solution was diluted in 10% HNO_3 aqueous solution before being analyzed by ICP-OES. X-ray photoelectron spectroscopy (XPS) measurements were carried out using a Kratos AXIS ULTRA^{DLD} XPS system equipped with an Al K_α monochromated X-ray source and a 165 mm electron energy hemispherical analyzer. The vacuum pressure was kept at <3 × 10^{-9} Torr during the measurements and a neutralizer was applied to compensate the charging issue during the measurement. All the XPS spectra were referenced to the C 1s peak at 284.8 eV of the surface adventitious carbon.

2.3. Electrochemical Measurements. Electrochemical properties were evaluated in symmetrical two-electrode Swagelok cells with 0.1 M K_2SO_4 and 8 M LiCl as the electrolytes. The working electrode was prepared by a homogeneous mixture of active material (V_2O_5/TiO_2), carbon black (99.9%; Alfa Aesar), and a solution of Poly(vinylidene

DOI: 10.1021/acsami.6b03569
ACS Appl. Mater. Interfaces 2016, 8, 12871−12880

Table 1. Measured Vanadium Content (V:Ti Atomic Ratio Measured From ICP), BET Surface Area, Nominal Surface Coverage, And Specific Capacitance of Six Samples Equilibrated at Different Temperatures with Three Different Types of 2-D Surface Vanadia Phases, Measured at Six Different Scan Rates[a]

annealing temperature (°C)	V:Ti atomic ratio (ICP)	BET surface area (m^2/g)	average pore size (nm)	nominal surface coverage (# of V atom/nm^2)	specific capacitance ($F/g_{v_2O_5}$) scan rate = 5 mV/s	20 mV/s	50 mV/s	100 mV/s	200 mV/s	500 mV/s
250 (submonolayer)	16.3	112.4	13.0	3.89	109.38	51.23	23.23	12.92	8	5.23
400 (monolayer)	14.2	87.5	14.3	5.68	137.47	98.8	50.8	26.83	14.8	7.68
450 (monolayer)	13.7	89.5	17.2	5.77	122.18	84.36	48.46	26.28	14.23	6.28
500 (monolayer)	17.8	70.4	19.6	5.64	120.33	85.83	48.67	28.67	17.17	8.83
550 (SAF)	13.8	32.4	26.3	15.73	102.34	88.96	71.17	55.45	40.26	21.3
600 (SAF)	14.3	6.3	63.0	77.66	81.62	73.78	64.73	57.57	49.19	33.51

[a]Nominal surface coverages were estimated from measured V:Ti ratio and BET surface area, assuming spherical particles.

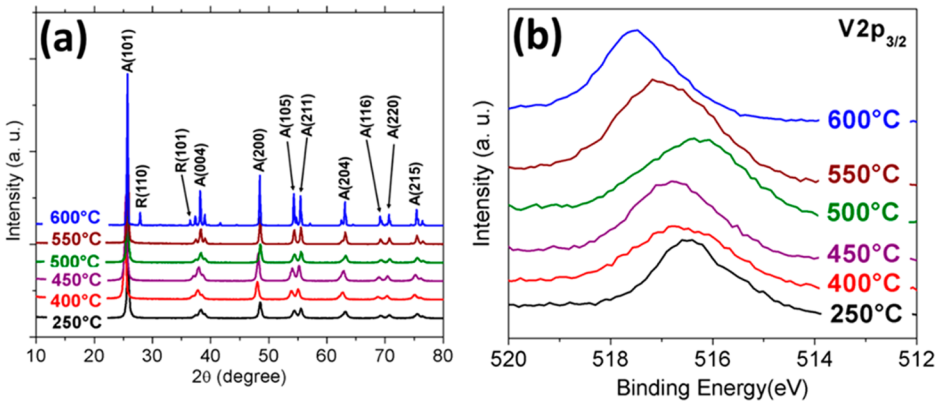

Figure 2. (a) X-ray diffraction (XRD) patterns of specimens annealed at different temperatures. Anatase and rutile phases are labeled by A and R respectively. No peaks related to vanadium oxides were observed. (b) XPS spectra of V $2p_{3/2}$ peaks for specimens equilibrated at different temperatures, confirming the presence of surface vanadium species for all cases.

fluoride) (PVDF) (Sigma-Aldrich) in *N*-methyl-2-pyrrolidone (NMP) as the binder (Alfa Aesar), at a weight ratio of 80:10:10. The mixture was uniformly pasted on a Ni foam using a painting brush, followed by drying at 120 °C in vacuum for 8 h. Celgard 3501 membrane was used as separator. The electrochemical properties and capacitance measurements of the samples were studied by cyclic voltammetry (CV) on a Solartron 1287 Potentiostat/Galvanostat. The following equation was used in order to determine the specific capacitance values by using the cyclic voltammetry method:

$$C = \int_{E_1}^{E_2} i(E)\mathrm{d}E/(E_2 - E_1)m\nu \tag{3}$$

where C is the specific capacitance of individual sample. E_1 and E_2 are the cutoff potentials in cyclic voltammetry, and $i(E)$ is the instantaneous current. The integral $\int_{E_1}^{E_2} i(E)\mathrm{d}E$ is the total charge obtained by integration of positive and negative sweep in cyclic voltammetry. $(E_2 - E_1)$ is the potential window width. m is the amount of vanadium loaded on each electrode. Galvanostatic constant current charge−discharge was performed in symmetric configuration of Swagelok cells at 600 mA/g using an Arbin tester. The average specific capacitance can be evaluated using the following equation:

$$C = 4(I\Delta t)/(m\Delta V) \tag{4}$$

where C is the specific capacitance, I is the discharging current (A), Δt is the discharging time, ΔV is the discharging voltage, and m is the mass of active material. Electrochemical Impedance Spectroscopy (EIS) was carried out using Solartron 1287 electrochemical interface coupled with a Frequency Response Analyzer (1255B) with an AC amplitude of 10 mV and a frequency range of 1 MHz to 2 mHz at open circuit potential of each sample. All the electrochemical studies described above were performed at room temperature (~25 °C).

3. RESULTS

3.1. Characterization of V_2O_5 Coated TiO_2 Nanoparticles. As being expected, the measured Brunauer−Emmett−Teller (BET) surface area of TiO_2 nanoparticles decreases with increasing annealing temperature due to nanoparticle coarsening (Figure 1a). Specifically, increasing the annealing temperature from 250 °C to 400, 450, and 500 °C, respectively, reduces the surface area from 112.4 m^2/g to 87.5, 89.5, and 70.4 m^2/g, respectively, representing ~20−37% reductions. Moreover, the surface area is further reduced by 71% to 32.4 m^2/g, when the annealing temperature is increased to 550 °C. Finally, annealing at 600 °C further reduces the surface area by as much as 94% to only 6.3 m^2/g. The reductions of surface areas are clearly evident in nitrogen adsorption−desorption isotherms (Figure 1b), where all the samples, except for the one annealed at the highest temperature of 600 °C, exhibit a typical type IV absorption behavior with distinct hysteresis loops that are characteristic of mesoporous and macroporous materials, and the measured pore size also increases with increasing annealing temperature (Table 1). The coarsening processes can also be evident by the narrowing of X-ray diffraction (XRD) peaks for the specimens with increasing annealing temperatures (Figure 2a). No vanadium oxide peak was observed for any specimens; low-intensity XRD peaks attributed to the formation of minor TiO_2 rutile phase are observed only in the specimen annealed at 600 °C, but absent for all other specimens annealed at lower temperatures.

3.2. Formation of 2-D Surface Vanadia Phases at Different Equilibration Temperatures. While the surface

DOI: 10.1021/acsami.6b03569
ACS Appl. Mater. Interfaces 2016, 8, 12871−12880

area of TiO_2 nanoparticles decreases, submonolayers, monolayers or multilayers (SAFs) of surface vanadia species form in sequence at thermodynamic equilibria with increasing equilibration temperature (Figure 1a). High resolution transmission electron microscopy (HRTEM) shows that nanometer-thick, V_2O_5-based SAFs form on the surfaces of the TiO_2 nanoparticles annealed at 550 and 600 °C (Figure 3a); the corresponding measured means of, and standard deviations in, the SAF thicknesses are plotted in Figure 1a, which are based on the measurements conducted in a prior systematic HRTEM study.[19,20] The surface vanadia species formed at 500 °C or lower temperatures are below the detection limit of HRTEM (Figure 3b); however, the formation of monolayer and submonolayer surface vanadia species upon annealing at 250−500 °C has been well established by extensive prior studies of supported monolayer catalysts,[12−17] and it is further verified by our X-ray photoelectron spectroscopy (XPS) results shown in Figure 2b. Furthermore, XPS results indicate that the binding energy of vanadium species shifts toward the higher end, especially with SAF formation at 550 and 600 °C, as comparing with the ones annealed at lower temperatures, suggesting higher oxidation states of vanadium that may affect the capacitance.

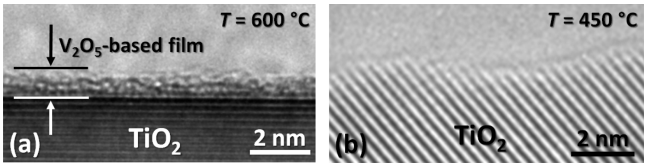

Figure 3. (a) Representative, nanometer-thick, vanadia-based SAF formed on TiO_2 in a specimen annealed at 600 °C. (b) Representative "clean" surface of TiO_2 nanoparticles for specimens equilibrated at 250−500 °C (450 °C for this specific case), where monolayers (or submonolayers) of 2-D surface vanadia phases are not discernible in HRTEM but have been detected by XPS (Figure 2b).

3.3. Electrochemical Performance of Different 2-D Surface Vanadia Phases. As shown in Figure 4a,b, the integrated areas of CV plots for pure TiO_2 at both 5 and 100 mV/s are significantly smaller than the nanoparticles with

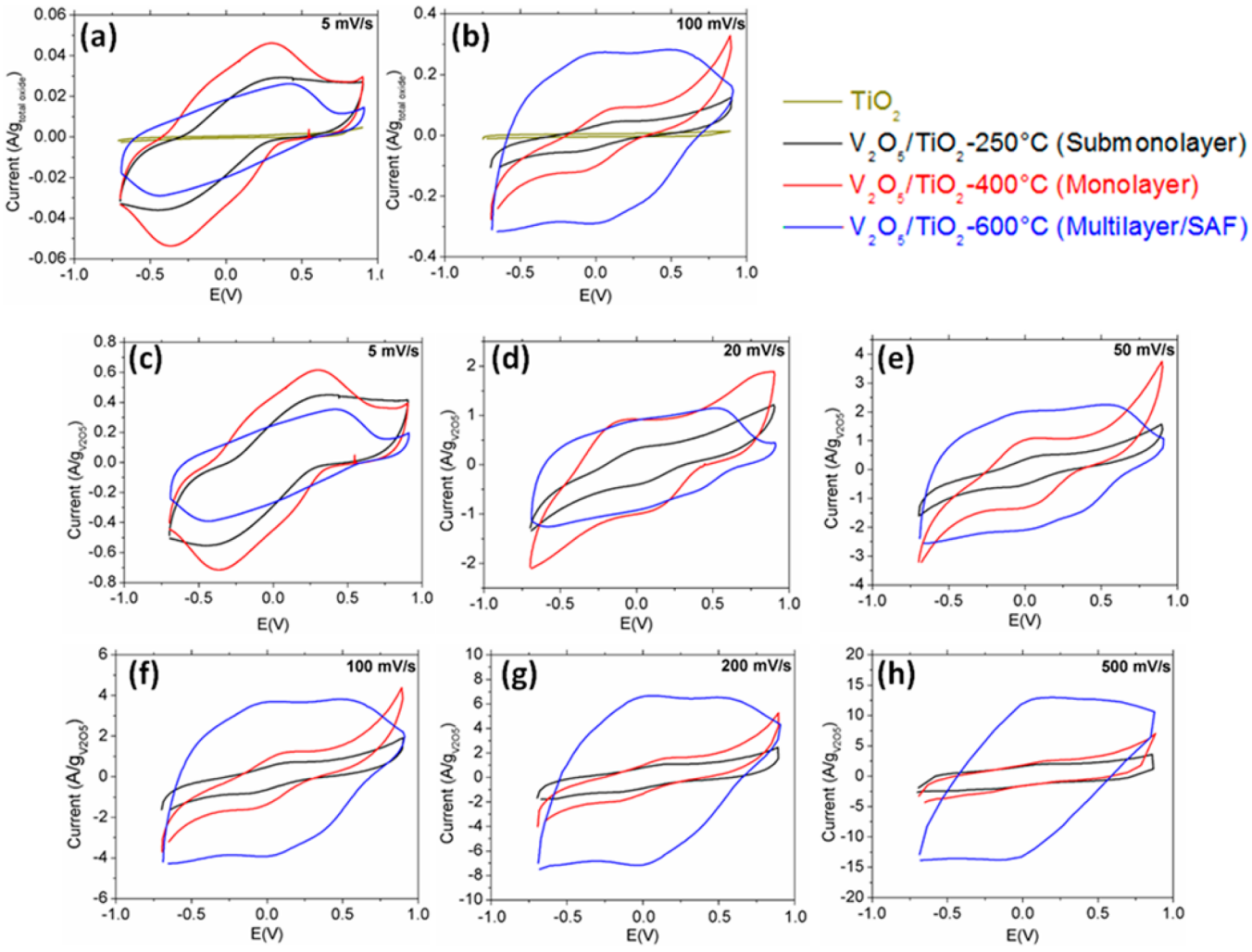

Figure 4. Cyclic voltammograms of pure TiO_2 nanoparticles and nanoparticles with 2-D surface vanadia phases, normalized to per gram of total oxide, measured at the scan rates of (a) 5 mV/s and (b) 100 mV/s in 0.1 M K_2SO_4 electrolyte. Cyclic voltammograms of three representative specimens, normalized per gram of vanadia, measured at the scan rates of (c) 5 mV/s, (d) 20 mV/s, (e) 50 mV/s, (f) 100 mV/s, (g) 200 mV/s, and (h) 500 mV/s in 0.1 M K_2SO_4 electrolyte, respectively. Additional data are reported for all six specimens equilibrated at 250, 400, 450, 500, 550, and 600 °C in Figures S1−S6 in the Supporting Information (and the data of only three representative specimens are displayed here for figure clarity).

DOI: 10.1021/acsami.6b03569
ACS Appl. Mater. Interfaces 2016, 8, 12871−12880

surface vanadia (and essentially negligible), confirming that the capacitances are mostly from the 2-D surface vanadia species.

Moreover, Figure 4c–h illustrates that the specimen equilibrated at 400 °C (with surface vanadia monolayers) has the highest capacitances at low scan rates of 5 and 20 mV/s, while the specimen equilibrated at 600 °C (with nanoscale SAFs; Figure 3a) has the highest capacitances at higher scan rates of 100–500 mV/s. Although some resistive behaviors are observed for nanoparticles with surface vanadia specimens at submonolayer and monolayer levels at 100 mV/s or higher scan rates, the CV plots for the specimens with multilayers/SAFs are not distorted at these high scan rates. For figure clarity, CV plots of only three representative specimens with three different types of surface vanadia phases are displayed in Figure 4; additional CV plots for all six specimens measured at six different scan rates are documented in Figures S1–S6 in the Supporting Information.

Specific capacitances of six different specimens with different 2-D surface vanadia phases measured at six different scan rates (from 5 to 500 mV/s) were calculated, and the results are plotted in Figure 5a for comparison. At the lowest scan rate of 5 mV/s, the formation of full monolayers (via increasing the equilibration temperature from 250 to 400 °C) improves the specific capacitance by 25% to ~137 F/$g_{v_2O_5}$ (despite a ~22% reduction in measured BET surface area). Further increasing the equilibration temperature beyond 400 °C will reduce the specific capacitance per gram of active material gradually at this low scan rate of 5 mV/s, which is due to the reduction of surface area; Figure 5b further shows that the measured capacitance per BET surface area is virtually constant in the monolayer region regardless of the annealing temperatures and in fact increases with the SAF formation at higher temperatures.

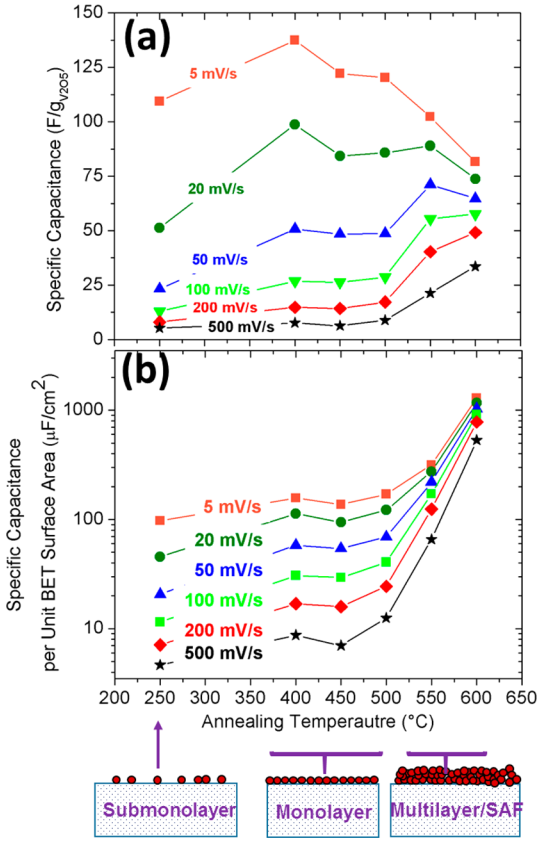

Figure 5. (a) Specific capacitance vs the equilibration temperature curves, measured at six different scan rates in 0.1 M K_2SO_4 electrolyte. Configurations of 2-D surface vanadia phases formed at these equilibrated temperatures are schematically illustrated. (b) Measured specific capacitances per unit BET surface area of specimens annealed at different temperatures and tested at six different scan rates.

At high scan rates, the specific capacitance increases monotonically with increasing the equilibration temperature; for example, at a scan rate of 200 mV/s, the measured specific capacitances are 8, 14.8, 14.23, 17.17, 40.26, and 49.19 F/$g_{v_2O_5}$, respectively, for the specimens annealed at 250, 400, 450, 500, 550, and 600 °C, respectively. This dependence on equilibration temperature is more significant for the measured specific capacitances per BET surface areas, as shown in Figure 5b.

Cycling stability of specimens with different 2-D surface vanadia phases, measured at a constant current of 600 mA/$g_{\text{total oxide}}$, in 0.1 M K_2SO_4 electrolyte is shown in Figure 6a. The gradual decaying of capacitances during the cycling is presumably due to the dissolution of vanadia into K_2SO_4 electrolyte, and it can be mitigated by using other types of electrolytes. To demonstrate the feasibility of improved cycling stabilities, a significantly improved cycling performance with ~96% retention after 500 cycles was observed for the specimen annealed at 600 °C in an 8 M LiCl electrolyte (Figure 6b). Yet, 0.1 M K_2SO_4 (instead of 8 M LiCl) electrolytes were used in most of this study to test the intrinsic pseudocapacitive properties of 2-D surface vanadia phases to avoid complexity due to the possible intercalation of Li^+ ions into underneath TiO_2 particles.

The galvanic constant current charge–discharge curves (measured at 600 mA/$g_{\text{total oxide}}$) in 0.1 M K_2SO_4 are shown in Figure 7 where the deviations from ideal triangular shapes can be attributed to pseudocapacitive reactions due to 2-D surface vanadia phases (presumably involving subsurface redox reactions). The charge–discharge curves of the specimens with nanoscale SAFs are largely symmetric and they are prolonged over the specimens with submonolayers and monolayers of surface vanadia, revealing good capacitive behaviors.

Nyquist plots of AC impedance of all six specimens are shown in Figure 8. The specimens with submonolayers and monolayers of surface vanadia display two semicircles at high- and midfrequencies (with large second semicircles at midfrequencies), followed by spikes in low frequency regions, whereas the specimens with nanoscale SAFs exhibit typical pseudocapacitive behaviors with small semicircle at high frequencies, followed by spikes at midfrequencies, as shown in the inset of Figure 8.

4. DISCUSSION

A series of prior studies[15,19,20] have already demonstrated that a variety of 2-D vanadia phases, particularly the monolayers and nanoscale surficial films (a.k.a. disordered multilayer adsorbates or SAFs), can form on the surfaces of titania spontaneously at thermodynamic equilibria through facile, cost-effective, and scalable mixing and annealing processes. Once the thermodynamic equilibria are achieved, the surface configuration and absorption amount (i.e., the surface V coverage or the effective thickness of the surficial film) should be independent of synthesis procedure/history but is a function of the equilibration temperature.

DOI: 10.1021/acsami.6b03569
ACS Appl. Mater. Interfaces 2016, 8, 12871–12880

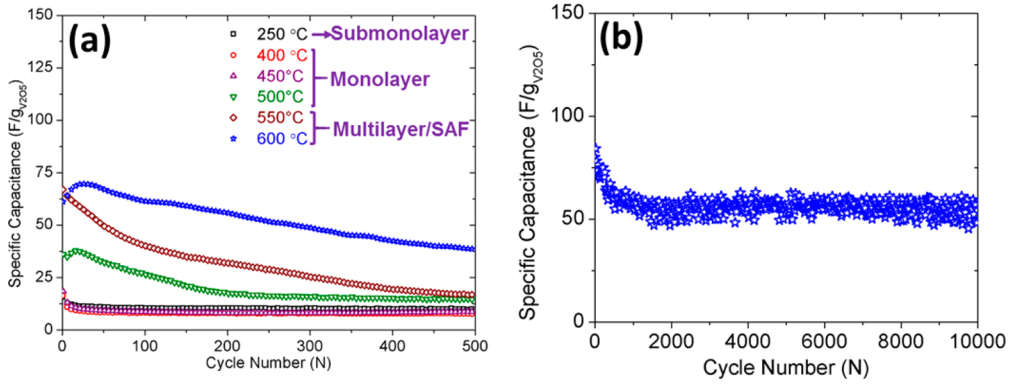

Figure 6. (a) Cycling stabilities of six different specimens (equilibrated at six different temperatures with three different types of 2-D surface vanadia phases) tested at a constant current of 600 mA/g in 0.1 M K_2SO_4. (b) Cycling stability of specimen with multilayer/SAF 2-D surface phase in an 8 M LiCl electrolyte, showing that the decaying of capacitance during cycling as a result of dissolution of vanadia in 0.1 M K_2SO_4 solution can be mitigated by using other types of electrolytes to reduce and prevent the dissolution of vanadia species.

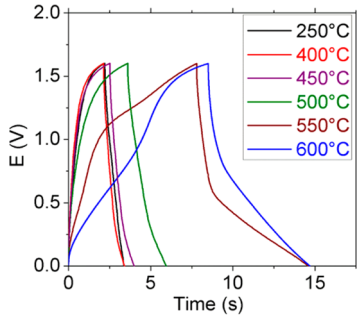

Figure 7. Comparison of galvanostatic constant current charge–discharge curves of different specimens annealed at different temperatures measured at 600 mA/$g_{total\ oxide}$ in 0.1 M K_2SO_4 electrolyte.

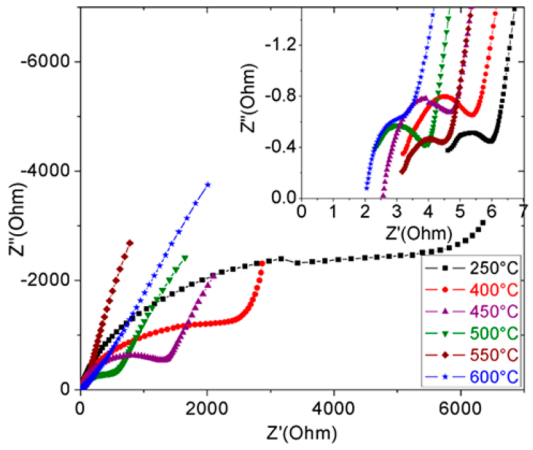

Figure 8. AC impedance plots of these six specimens. The inset shows the semicircles for these six samples at high frequencies (in an expanded view near the origin point).

Specifically, a nanometer-thick vanadia-based surficial film can form spontaneously at sufficiently high temperatures (550–600 °C in this case), driven by the reduction of surface energy:

$$\Delta\gamma \equiv \gamma_{\text{vanadia}} + \gamma_{\text{vanadia-titania}} - \gamma^{(0)}_{\text{titania}} < 0 \qquad (1)$$

where h is the film thickness and γ's are interfacial energies.[9,19,20] Moreover, these nanoscale surficial films or SAFs appear to be largely disordered in HRTEM (Figure 3a) because the formation of crystalline surface vanadia films is frustrated by the high crystal-to-crystal interfacial energy that would occur, although existence of partial orders in such surficial films is confirmed (even if they are named as surface "amorphous" films or SAFs).[19,20]

The stabilization of a subsolidus, quasi-liquid, surficial films (SAFs) can be conceived as if the increased free energy for forming the undercooled liquid film ($\Delta G^{(\text{vol.})}_{\text{amorph.}}\cdot h$) is over-compensated by $-\Delta\gamma$. In a pressure-balance model[9,19−21] that was adapted from the original Clarke model for equilibrium-thickness intergranular films,[22,23] the excess surface energy (referred to a "clean" titania surface without adsorption or $\gamma^{(0)}_{\text{titania}}$) can be expressed as

$$\Delta\sigma(h) = \Delta\gamma + \Delta G^{(\text{vol.})}_{\text{amorph.}}\cdot h + \sigma_{\text{vdW-Ld}}(h) + \sigma_{\text{elec.}}(h) + \sigma_{\text{short-range}}(h) + \ldots \qquad (2)$$

which includes the amorphization energy as well as the van der Waals London dispersion (vdW-Ld), electrostatic and short-range interfacial interactions. A surficial film may form spontaneously if $\Delta\sigma(h) < 0$, and the equilibrium thickness corresponds to a minimum in $\Delta\sigma(h)$.

The equilibrium thickness of the SAFs (a.k.a. disordered multilayer adsorbates) decreases with decreasing temperature because of the $\Delta G^{(\text{vol.})}_{\text{amorph.}}\cdot h$ term, which represents a constant attractive pressure that increases by ∼1 MPa/K (approximately the volumetric fusion entropy of V_2O_5) with reducing temperature.[20] Thus, the nanometer-thick vanadia-based surficial will transit ("collapse") to monolayers (via a first-order surface phase-like transformation) at ∼500 °C with a hysteresis loop (i.e., nanoscale SAFs form at ∼500 °C with increasing temperature but vanish at ∼450 °C with decreasing temperature).[20] Thus, monolayers of surface vanadia form in specimens equilibrated at 400–500 °C (Figure 1a), the formation of which are well expected from extensive prior studies of V_2O_5 on TiO_2 monolayer catalysts;[12−17] the presence of surface vanadia is also verified by our XPS results (Figure 2b). We further estimate the nominal surface coverages of vanadium for these specimens by using the measured BET surface areas and overall composition measured by ICP. As shown in Table 1, the nominal surface coverages are estimated to be 5.68, 5.77, and 5.64 V atom/nm^2, respectively, for specimens annealed at 400, 450, and 500 °C, respectively, which is close to the theoretical monolayer coverage of ∼8 V

DOI: 10.1021/acsami.6b03569
ACS Appl. Mater. Interfaces 2016, 8, 12871−12880

atoms per nm^2 (where the difference may be explained by the fact that surface vanadia has a different density).[17] The constant surface coverage (~5.6−5.8 V atom/nm^2) for specimens equilibrated in the temperature range of 400−500 °C is also an indication that an equilibrium monolayer coverage is reached at this plateau. In contrast, the nominal vanadium surface coverage is estimated to be 3.89 V atom/nm^2 for the specimen annealed at 250 °C, indicating the formation of submonolayers.

Compared with the recent study of Epifani et al. (of the pseudocapacitive properties of V_2O_5-based submonolayers formed at a lower temperature of 250 °C),[18] the current study illustrated that surface monolayers perform better at all scan rates; moreover, SAFs/multilayers perform significantly better at thigh scan rates. Specifically, using three electrodes cells, Epifani et al. recently reported a specific capacitance of 125 F/$g_{v_2O_5}$ at a low scan rate 5 mV/s for a sample annealed at 250 °C (with submonolayers),[18] which is close to the value obtained in this investigation (~109 F/$g_{v_2O_5}$). A slight difference between the two values can be attributed either to the differences in electrode preparation procedures or different cell setups. However, cyclic voltammetry at higher scan rates has not been studied in that prior report,[18] although higher scan rates are of crucial importance for supercapacitor applications (as discharging within ~1 min corresponds to typical scan rates of 20−40 mV/s).[24] This study showed that the measured capacitance for the submonolayer specimen (annealed at 250 °C) decreases rapidly with increasing scan rates in the range of 20 to 500 mV/s (Figure S7); specifically, it decreases from ~109 F/$g_{v_2O_5}$ at 5 mV/s to ~23 F/$g_{v_2O_5}$ at 50 mV/s and only ~5 F/$g_{v_2O_5}$ at 500 mV/s, which represent only ~20% (at the 10× scan rate) and ~5% (at the 100× scan rate), respectively, of the capacitance measured at the slow scan rate of 5 mV/s. As we will discuss in detail later, the lower high-rate performance may be related to diffusion-controlled process in this specimen. In the case of specimen with complete monolayer (annealed at 500 °C), the measured capacitance decreases rapidly with increasing scan rates in the range of 50 to 500 mV/s (Figure S7); specifically, it decreases from ~120 F/$g_{v_2O_5}$ at 5 mV/s to 48 F/$g_{v_2O_5}$ at 50 mV/s and only 8 F/$g_{v_2O_5}$ at 500 mV/s, which represents 40% (at the 10× scan rate) and 6% (at 100× scan rate), respectively, of the capacitance measured at the low scan rate of 5 mV/s. In contrast, for the specimen annealed at 600 °C with SAF formation, the measured capacitance decreases from ~82 F/$g_{v_2O_5}$ at 5 mV/s to ~65 F/$g_{v_2O_5}$ at 50 mV/s and ~34 F/$g_{v_2O_5}$ at 500 mV/s, which represent ~79% (at the 10× scan rate) and ~41% (at the 10× scan rate), respectively (Figure S7).

All three specimens with monolayers of surface vanadia (formed at 400−500 °C, with ~5.6−5.8 vanadium atoms per nm^2; Table 1) exhibit similar capacitances at each scan rates (Figure 3a and Table 1, as well as Figure 3b for capacitances normalized to per unit BET surface area), which outperforms the specimen with submonolayer surface vanadia formed at a lower temperature of 250 °C (with ~3.9 vanadium atoms per nm^2; Table 1), despite ~20−37% reductions in BET surface areas after annealing at higher temperatures (Figure 1a).

Moreover, the specimen with nanoscale SAF formation (multilayer vanadia adsorbates; see Figure 5a and Figure 6a) outperformed specimens with submonolayers and monolayers of surface vanadia at moderate and high scan rates of 50−500 mV/s. To benchmark the pseudocapacitive properties of 2-D surface vanadia phases, we first compare them with electrospun V_2O_5 fibers. Specific capacitances of nanoscale SAFs are significantly higher than those reported for electrospun V_2O_5 nanofibers of ~500−800 nm in diameters (tested in $LiPF_6$ in EC/DEM),[25] particularly at high scan rates (e.g., ~5−6× at 50−100 mV/s) but are ~20% lower than the K-intercalated layered V_2O_5 nanofibers of ~120 nm in diameters (with ~20 wt % C added, tested in a more concentrated electrolyte of 2 M KCl);[26] noting that quantitative comparisons may be difficult because different electrolytes and carbon loading (and a low electrolyte concentration of 0.1 MK_2SO_4 and relative low carbon loading of 10 wt % were used in this study to probe the intrinsic pseudocapacitive properties of 2-D surface vanadia phases). However, the capacitances are still significantly lower than nanometer-thick V_2O_5 coated on mesoscale ITO scaffold[27] or mesoscale ITO scaffold[28] via atomic layer deposition (ALD) or other sophisticated synthesis routes with fine processing controls; the differences are presumably due to the much high conductivities of ITO and carbon nanotubes. Yet, the 2-D surface vanadia phases can form spontaneously via on abundant TiO_2 nanoparticle supports via a cost-effective and scalable synthesis method (that can be extended to many other materials systems), thereby having advantages in both cost and manufacturability.

Here, the scalability and potential low costs are related to the fact that TiO_2 nanoparticles have already been produced cost-effectively in a large scale; furthermore, the proposed V_2O_5/TiO_2 supercapacitor electrode materials can be fabricated via simply mixing and annealing cheap TiO_2 nanoparticles with V-containing salts, which can (again) be done in a large-scale production easily (as the petroleum industry is already doing for making V_2O_5/TiO_2-based catalysts). In addition, V_2O_5/TiO_2 is only one of the possible systems and there are many other existing (or potentially new) oxide systems that form similar (or even different types of) 2-D surface phases, which may have good/better electrochemical properties and should be explored in future studies.

This study also reveals some intriguing and fascinating scientific findings about pseudocapacitive properties of 2-D surface vanadia phases. An interesting observation from Figure 5 and Table 1 is at the higher scan rates of 50−500 mV/s, the measured capacitances generally increase with increasing annealing temperature, despite of the significant reductions of BET surface areas. Take the measurements conducted at the scan rates of 100 mV/s as an example, the measured capacitance is ~13 F/$g_{v_2O_5}$ for the specimen equilibrated at 250 °C with an BET surface area of ~112 m^2/g. After annealing at 400−500 °C, the BET surfaces areas are reduced by ~20−37% to ~70−90 m^2/g with the formation of monolayers, but the measured capacitances increase by >280% to ~49−51 F/$g_{v_2O_5}$. Furthermore, after annealing at 550 and 600 °C, the BET surfaces areas are further reduced by ~71% and ~94% to ~32 and ~6 m^2/g, respectively, with the formation of nanoscale SAFs, but the measured capacitances further increase by >300% (>4×) to ~55−59 F/$g_{v_2O_5}$. These results are in contrast with numerous previous reports of higher specific capacitances for materials with higher specific surface areas for both electric double layer capacitance[29−31] as well as pseudocapacitance materials.[32−34] Nonetheless, the somewhat unusual behaviors at high scan rates can be explained by charge transfer processes. Specifically, in specimens with submonolayer and monolayer 2-

DOI: 10.1021/acsami.6b03569
ACS Appl. Mater. Interfaces 2016, 8, 12871−12880

D surface phases with high surface areas, the interaction of electrolyte and TiO_2 nanoparticles becomes more significant compared with specimen with multilayers/nanometer-thick SAFs which has a much lower surface area. The small semicircles observed at high frequencies in Nyquist plots of all specimens are due to the electrode/electrolyte interface (electrode resistance) which is also very similar for different specimens with different 2-D surface phases. However, specimens annealed at 250−500 °C exhibit additional large semicircles at midfrequencies, whose diameters are correlated with the surface area of the specimens. The specimen with submonolayers and highest surface area has the highest charge transfer resistance and specimens with monolayers with lower surface area has smaller charge transfer resistance while the specimens with multilayers/nanoscale SAFs have a very small charge transfer resistance. The charge transfer resistance is known to be correlated with the surface area and conductivity of the active material.[35]

Improvements in redox reaction kinetics and electrochemical activity are also evident for specimens with formation of nanoscale SAFs, as compared with specimens with submonolayers and monolayers of 2-D surface vanadia phases, which are indicated by the shifts of the onset potential of oxidation peaks in Figure 4 and Figures S1−S6. This is also in agreement with the XPS results (Figure 2b), where a chemical shifts toward the high-energy end indicates higher oxidation states of vanadium with higher concentrations of 5+ vanadium cations with the formation of nanoscale SAFs. It has been reported that fully oxidized V (5+) surface VO_x species are more efficient for redox reactions.[36] DFT calculations has also shown that loading vanadium oxide on titania results in band gap reduction improving the electronic properties of vanadium oxide which can lead to possible change in the reactivity of the catalyst.[37] Band gap engineering is shown to improve the electrical properties of materials for supercapacitor applications.[38]

The significantly better performances of specimens with nanoscale SAFs at high scan rates, as compared with specimens with monolayers of surface vanadia phases, also suggest possible subsurface redox reactions, which may be facilitated by the fact that these nanoscale SAFs are partially ordered with more open structures than the normal glasses;[9,19,20] a recent study showed that such partially ordered and partially disordered SAFs strained on curved surfaces may enhance the ionic transport in nanowires,[6] and it is possible that a similar effect may promote ion transport and enable/enhance subsurface redox reaction in the current case.

Finally, it should be noted that this study intentionally used low vanadium contents (where all vanadia species are on the surfaces) to ensure the measurements of intrinsic behaviors of 2-D surface vanadia species. Using higher vanadium contents can further increase the specific capacitance per total oxides.[39] In addition, both the specific capacitance and the cycling stability can be further improved by using different types of electrolytes, as shown in a previous report[40,41] as well as demonstrated in Figure 6b of this study. The primary scientific goal of this study is to understand the pseudocapacitive properties of 2-D surface vanadia species (vs optimizing the whole system) as an example to demonstrate the potential of 2-D surface phases. Yet, this study demonstrated that the pseudocapacitive properties of vanadia-based nanoscale SAFs supported on TiO_2 are significantly better that those of the submonolayer vanadia adsorbates reported in a recent pioneering study by Epifani et al. that first pinpointed the possibility of utilizing surface vanadia species as pseudocapacitors,[18] particularly in the moderate and high capacitance regions (20−500 mV/s) that are of practical importance. We again emphasize that such 2-D surface vanadia species can form spontaneously (via a facile and scalable "mixing and annealing" process) on the surfaces of the abundant TiO_2 anatase nanoparticles, which can be produced cost-effectively in a large quantity; the relevant synthesis and processing routes via utilizing spontaneously formed 2-D surface phases (that can be extended to many other materials systems) are generally economic and have excellent scalability and manufacturability.

5. CONCLUSION

In summary, we have investigated the pseudocapacitive properties of 2-D vanadia phases that form spontaneously on the surfaces of TiO_2 nanoparticles during annealing. Annealing at low temperatures (<300 °C) results in high surface area nanoparticles with submonolayers of 2-D surface vanadia and small pore sizes, with a good capacitance at a low scan rate of 5 mV/s decaying rapidly with increasing scan rate. Annealing at medium temperatures of 400−500 °C results in specimens with 20−37% lower surface areas and high surface V coverages of monolayers of 2-D vanadia, which improved specific capacitances per unit active material at all rates. Nanoscale surficial vanadia films (SAFs or multilayer adsorbates) form at high equilibration temperatures of 550−600 °C, which lead to significantly better performances at moderate and high scam rates (20−500 mV/s), despite the significant reduction of surface areas.

This study suggests a new direction to design and cost-effectively fabricate a novel class of supercapacitors based on 2-D surface adsorbates that can be made via facile and scalable synthesis routes. A related general scientific goal is to utilize 2-D interfacial phases to achieve distinct and unique properties, which has recently been demonstrated for lithium-ion batteries,[2−5] oxygen-ion conducting nanowires,[6] and photocatalysts;[7,8] this study further extends it to supercapacitors. The facile synthesis and processing routes via utilizing spontaneously formed 2-D surface phases can be further extended to various other materials systems with excellent scalability and manufacturability.

■ ASSOCIATED CONTENT

Supporting Information

The Supporting Information is available free of charge on the ACS Publications website at DOI: 10.1021/acsami.6b03569.

Cyclic voltammograms of samples annealed at different temperatures and the measured specific capacitance at different scan rates for samples annealed at different temperatures (PDF).

■ AUTHOR INFORMATION

Corresponding Author

*J. Luo. Email: jluo@alum.mit.edu.

Notes

The authors declare no competing financial interest.

■ ACKNOWLEDGMENTS

This work is financially supported in part by National Science Foundation under the grant no. DMR-1006515 for 2013−2015. J.L. also thanks partial support from a National Security Science and Engineering Faculty Fellowship (grant no. N00014-15-1-

DOI: 10.1021/acsami.6b03569
ACS Appl. Mater. Interfaces 2016, 8, 12871−12880

0030) after the completion of the NSF project. The authors thank Prof. Zaera and Dr. Lee at UC Riverside for XPS measurements with equipment supported by an NSF grant no. DMR-0958796. We thank Prof. Yu Qiao and Cang Zhao for providing BET measurement equipment and training and Dr. Haijun Qian for the HRTEM images shown in Figure 3 and the abstract graphic.

REFERENCES

(1) Cantwell, P. R.; Tang, M.; Dillon, S. J.; Luo, J.; Rohrer, G. S.; Harmer, M. P. Overview No. 152: Grain Boundary Complexions. *Acta Mater.* **2014**, *62*, 1−48.
(2) Wang, K. X.; Li, X. H.; Chen, J. S. Surface and Interface Engineering of Electrode Materials for Lithium-ion Batteries. *Adv. Mater.* **2015**, *27* (3), 527−545.
(3) Samiee, M.; Luo, J. A Facile Nitridation Method to Improve the Rate Capability of TiO_2 for Lithium-ion Batteries. *J. Power Sources* **2014**, *245*, 594−598.
(4) Huang, J. J.; Luo, J. A Facile and Generic Method to Improve Cathode Materials for Lithium-ion Batteries via Utilizing Nanoscale Surface Amorphous Films of Self-regulating Thickness. *Phys. Chem. Chem. Phys.* **2014**, *16* (17), 7786−7798.
(5) Kang, B.; Ceder, G. Battery Materials for Ultrafast Charging and Discharging. *Nature* **2009**, *458* (7235), 190−193.
(6) Liu, W.; Pan, W.; Luo, J.; Godfrey, A.; Ou, G.; Wu, H.; Zhang, W. Suppressed Phase Transition and Giant Ionic Conductivity in $La_2Mo_2O_9$ Nanowires. *Nat. Commun.* **2015**, *6*, 8354.
(7) Samiee, M.; Luo, J. Enhancing the Visible-light Photocatalytic Activity of TiO_2 by Heat Treatments in Reducing Environments. *Mater. Lett.* **2013**, *98*, 205−208.
(8) Chen, X. B.; Liu, L.; Yu, P. Y.; Mao, S. S. Increasing Solar Absorption for Photocatalysis with Black Hydrogenated Titanium Dioxide Nanocrystals. *Science* **2011**, *331* (6018), 746−750.
(9) Luo, J.; Chiang, Y.-M. Wetting and Prewetting on Ceramic Surfaces. *Annu. Rev. Mater. Res.* **2008**, *38*, 227−249.
(10) Zhao, Q. L.; Wang, X. Y.; Liu, J.; Wang, H.; Zhang, Y. W.; Gao, J.; Liu, J.; Lu, Q. Surface Modification and Performance Enhancement of Carbon Derived from Chromium Carbide for Supercapacitor Applications. *J. Electrochem. Soc.* **2015**, *162* (6), A845−A851.
(11) Candelaria, S. L.; Garcia, B. B.; Liu, D. W.; Cao, G. Z. Nitrogen Modification of Highly Porous Carbon for Improved Supercapacitor Performance. *J. Mater. Chem.* **2012**, *22* (19), 9884−9889.
(12) Wachs, I. E.; Saleh, R. Y.; Chan, S. S.; Chersich, C. C. The Interaction of Vanadium Pentoxide with Titania (Anatase) 0.1. Effect on O-Xylene Oxidation to Phthalic-Anhydride. *Appl. Catal.* **1985**, *15* (2), 339−352.
(13) Cavani, F.; Foresti, E.; Trifiro, F.; Busca, G. Nature of Active Species in the Ammoxidation of Toluene over V_2O_5/TiO_2 Catalysts Prepared by Flash-Drying. *J. Catal.* **1987**, *106* (1), 251−262.
(14) Sanati, M.; Andersson, A. Ammoxidation of Toluene over TiO_2(B)-Supported Vanadium-Oxide Catalysts. *J. Mol. Catal.* **1990**, *59* (2), 233−255.
(15) Xie, Y.-C.; Tang, Y.-Q. Spontaneous Monolayer Dispersion of Oxides and Salts onto Surfaces of Supports: Applications to Heterogeneous Catalysis. *Adv. Catal.* **1990**, *37*, 1−43.
(16) Wachs, I. E.; Weckhuysen, B. M. Structure and Reactivity of Surface Vanadium Oxide Species on Oxide Supports. *Appl. Catal., A* **1997**, *157* (1−2), 67−90.
(17) Wachs, I. E. Catalysis Science of Supported Vanadium Oxide Catalysts. *Dalton Trans.* **2013**, *42* (33), 11762−11769.
(18) Epifani, M.; Chavez-Capilla, T.; Andreu, T.; Arbiol, J.; Palma, J.; Morante, J. R.; Diaz, R. Surface Modification of Metal Oxide Nanocrystals for Improved Supercapacitors. *Energy Environ. Sci.* **2012**, *5* (6), 7555−7558.
(19) Qian, H.; Luo, J. Nanoscale Surficial Films and a Surface Transition in V_2O_5-TiO_2-based Ternary Oxide Systems. *Acta Mater.* **2008**, *56* (17), 4702−4714.
(20) Qian, H. J.; Luo, J. Vanadia-based Equilibrium-thickness Amorphous Films on Anatase (101) Surfaces. *Appl. Phys. Lett.* **2007**, *91* (6), 061909.
(21) Luo, J.; Tang, M.; Cannon, R. M.; Carter, W. C.; Chiang, Y.-M. Pressure-Balance and Diffuse-Interface Models for Surficial Amorphous Films. *Mater. Sci. Eng., A* **2006**, *422*, 19−28.
(22) Clarke, D. R.; Shaw, T. M.; Philipse, A. P.; Horn, R. G. Possible Electrical Double-Layer Contribution to the Equilibrium Thickness of Intergranular Glass Films in Polycrystalline Ceramics. *J. Am. Ceram. Soc.* **1993**, *76*, 1201−04.
(23) Clarke, D. R. On the Equilibrium Thickness of Intergranular Glass Phases in Ceramic Materials. *J. Am. Ceram. Soc.* **1987**, *70* (1), 15−22.
(24) Stoller, M. D.; Ruoff, R. S. Best Practice Methods for Determining an Electrode Material's Performance for Ultracapacitors. *Energy Environ. Sci.* **2010**, 3 (9), 1294−1301.
(25) Aravindan, V.; Cheah, Y. L.; Mak, W. F.; Wee, G.; Chowdari, B. V. R.; Madhavi, S. Fabrication of High Energy-Density Hybrid Supercapacitors Using Electrospun V2O5 Nanofibers with a Self-Supported Carbon Nanotube Network. *ChemPlusChem* **2012**, *77* (7), 570−575.
(26) Yeager, M. P.; Du, W. X.; Bishop, B.; Sullivan, M.; Xu, W. Q.; Su, D.; Senanayake, S. D.; Hanson, J.; Teng, X. W. Storage of Potassium Ions in Layered Vanadium Pentoxide Nanofiber Electrodes for Aqueous Pseudocapacitors. *ChemSusChem* **2013**, *6* (12), 2231−2235.
(27) Rauda, I. E.; Augustyn, V.; Saldarriaga-Lopez, L. C.; Chen, X.; Schelhas, L. T.; Rubloff, G. W.; Dunn, B.; Tolbert, S. H. Nanostructured Pseudocapacitors Based on Atomic Layer Deposition of V_2O_5 onto Conductive Nanocrystal-based Mesoporous ITO Scaffolds. *Adv. Funct. Mater.* **2014**, *24* (42), 6717−6728.
(28) Shakir, I.; Choi, J. H.; Shahid, M.; Shahid, S. A.; Rana, U. A.; Sarfraz, M.; Kang, D. J. Ultra-thin and Uniform Coating of Vanadium Oxide on Multiwall Carbon Nanotubes through Solution based Approach for High Performance Electrochemical Supercapacitors. *Electrochim. Acta* **2013**, *111*, 400−404.
(29) Salari, M.; Aboutalebi, S. H.; Konstantinov, K.; Liu, H. K. A Highly Ordered Titania Nanotube Array as a Supercapacitor Electrode. *Phys. Chem. Chem. Phys.* **2011**, *13* (11), 5038−5041.
(30) Xu, J. D.; Gao, Q. M.; Zhang, Y. L.; Tan, Y. L.; Tian, W. Q.; Zhu, L. H.; Jiang, L. Preparing two-dimensional microporous carbon from Pistachio nutshell with high areal capacitance as supercapacitor materials. *Sci. Rep.* **2014**, *4*, 5545.
(31) Park, S. H.; Yoon, S. B.; Kim, H. K.; Han, J. T.; Park, H. W.; Han, J.; Yun, S. M.; Jeong, H. G.; Roh, K. C.; Kim, K. B. Spine-like Nanostructured Carbon Interconnected by Graphene for High-performance Supercapacitors. *Sci. Rep.* **2014**, *4*, 6118.
(32) Zhu, T.; Zheng, S. J.; Chen, Y. G.; Luo, J.; Guo, H. B.; Chen, Y. E. Improvement of Hydrothermally Synthesized MnO_2 Electrodes on Ni Foams via Facile Annealing for Supercapacitor Applications. *J. Mater. Sci.* **2014**, *49* (17), 6118−6126.
(33) Zhu, Y. Q.; Cao, C. B.; Tao, S.; Chu, W. S.; Wu, Z. Y.; Li, Y. D. Ultrathin Nickel Hydroxide and Oxide Nanosheets: Synthesis, Characterizations and Excellent Supercapacitor Performances. *Sci. Rep.* **2014**, *4*, 5787.
(34) Yang, Q.; Lu, Z. Y.; Sun, X. M.; Liu, J. F. Ultrathin Co_3O_4 Nanosheet Arrays with High Supercapacitive Performance. *Sci. Rep.* **2013**, *3*, 3537.
(35) Salari, M.; Aboutalebi, S. H.; Chidembo, A. T.; Nevirkovets, I. P.; Konstantinov, K.; Liu, H. K. Enhancement of the Electrochemical Capacitance of TiO_2 Nanotube Arrays through Controlled Phase Transformation of Anatase to Rutile. *Phys. Chem. Chem. Phys.* **2012**, *14* (14), 4770−9.
(36) Zhao, C. L.; Wachs, I. E. Selective Oxidation of Propylene over Model Supported V2O5 Catalysts: Influence of Surface Vanadia Coverage and Oxide Support. *J. Catal.* **2008**, *257* (1), 181−189.
(37) Alexopoulos, K.; Hejduk, P.; Witko, M.; Reyniers, M. F.; Marin, G. B. Theoretical Study of the Effect of (001) TiO_2 Anatase Support on V_2O_5. *J. Phys. Chem. C* **2010**, *114* (7), 3115−3130.

DOI: 10.1021/acsami.6b03569
ACS Appl. Mater. Interfaces 2016, 8, 12871−12880

(38) Saha, S.; Jana, M.; Khanra, P.; Samanta, P.; Koo, H.; Murmu, N. C.; Kuila, T. Band Gap Engineering of Boron Nitride by Graphene and Its Application as Positive Electrode Material in Asymmetric Supercapacitor Device. *ACS Appl. Mater. Interfaces* **2015**, *7* (26), 14211−14222.
(39) Hu, C. C.; Xu, H. H.; Liu, X. X.; Zou, F.; Qie, L.; Huang, Y. H.; Hu, X. L. VO_2/TiO_2 Nanosponges as Binder-Free Electrodes for High-Performance Supercapacitors. *Sci. Rep.* **2015**, *5*, 16012.
(40) Boukhalfa, S.; Evanoff, K.; Yushin, G. Atomic Layer Deposition of Vanadium Oxide on Carbon Nanotubes for High Power Supercapacitor Electrodes. *Energy Environ. Sci.* **2012**, *5* (5), 6872−6879.
(41) Wang, G. M.; Lu, X. H.; Ling, Y. C.; Zhai, T.; Wang, H. Y.; Tong, Y. X.; Li, Y. LiCl/PVA Gel Electrolyte Stabilizes Vanadium Oxide Nanowire Electrodes for Pseudocapacitors. *ACS Nano* **2012**, *6* (11), 10296−10302.

DOI: 10.1021/acsami.6b03569
ACS Appl. Mater. Interfaces 2016, 8, 12871−12880